Published in final edited form as:
Chem Sci. 2011 ; 2(6): 1080–1085. doi:10.1039/C0SC00637H.

All-optical fluorescence image recovery using modulated Stimulated Emission Depletion

Chaoyang Fan[a], **Jung-Cheng Hsiang**[a], **Amy E. Jablonski**[a], and **Robert M. Dickson**[a]

Robert M. Dickson: dickson@chemistry.gatech.edu

[a]School of Chemistry and Biochemistry, and Petit Institute for Bioengineering and Bioscience, Georgia Institute of Technology, Atlanta, GA 30332-0400, USA. Fax: 404 385-6048; Tel: 404 894-4007

Abstract

Fluorescence modulation for selective recovery of desired fluorescence signals has to date required careful fluorophore selection combined with repeated optical recovery from long-lived photoinduced dark states. Adapting an all-optical scheme, modulated Stimulated Emission Depletion generalizes such modulation schemes by eliminating the need for dark state residence by directly optically depopulating the emissive state at any externally applied frequency. Using two overlapped Gaussian laser spots with the depletion beam being intensity-modulated, fluorescence modulation is readily achieved with a depletion ratio governed by the intensity of the depleting laser. Selective image recovery of otherwise unmodulatable fluorophore signals is directly achieved through this all-optical modulation, and common STED-degrading multiphoton-excited background is readily discriminated against. Both beads and dyes in solution as well as fluorophores bound within fixed cells are readily imaged in this manner.

I. Introduction

Fluorescence microscopy enables detailed studies of both biological dynamics and structure, but selective detection, especially in high background[1–4] or intracellular conditions, [5–10] often poses significant challenges. Absorption spectroscopy has addressed sensitivity concerns through either laser or molecular modulation,[11–13] the latter of which preferentially and repetitively alters the absorption signal of the species of interest relative to background.[13] Either changing the laser intensity at the absorption frequency or spectrally modulating the molecular resonance relative to the laser results in modulation of the transmitted laser intensity. Repeated application of this spectral modification at a very specific frequency moves the desired signal from zero frequency to the externally applied modulation frequency, while only the greatly reduced background within the very narrow detection bandwidth contributes to the noise. Fluorescence spectroscopy, however, is often considered a zero background technique,[14–15] as the excitation source is filtered out to leave only the desired molecular fluorescence. Unfortunately, the incredible complexity of biological systems presents a wide variety of natural emitters giving non-specific background that can obscure signals of interest.[1–5, 16–19] The challenge, then, is to preferentially recover the desired signal, minimizing contribution from the background.

Building on photoswitch-based optical lock-in detection (OLID)[3] that cross-correlates exogenous reference dye signals to extract reversibly photoswitched fluorescence, we designed methods of encoding any external modulation waveform on the fluorescence of

Correspondence to: Robert M. Dickson, dickson@chemistry.gatech.edu.

specific emitters without introduction of a reference dye signal.[20–21] In contrast to OLID, the secondary laser in Synchronously Amplified Fluorescence Recovery (SAFIRe) is lower energy than that of the collected fluorescence, thereby generating no additional background and more readily distinguishing fluorescence of interest from that of background emitters.[20–21] Such fluorescence modulation enables selective fluorescence recovery through demodulation (or selective detection) at the applied external modulation frequency, completely analogous to molecular modulation schemes.[20–21] In SAFIRe, the optical depopulation of transient fluorophore dark states with a secondary laser operating at lower energy than that of the detected fluorescence selectively and dynamically increases fluorophore emission, without altering the background. Demodulation at the applied modulation frequency then selectively recovers the weak target fluorescence, independent of background, by selectively detecting only the signal of interest.

Such selective fluorescence signal recovery using optical modulation has been successfully demonstrated with Ag nanodots, through optically-induced dark state depopulation.[20] Occurring under near-IR illumination, ~10-μsec-lived metastable dark states are more rapidly depopulated than by natural decay, thereby optically enhancing fluorescence at higher energy than that of the secondary illumination. Recent efforts have extended these lessons in Ag nanodot modulation to a series of xanthene dyes,[21] and most recently by optically inhibiting FRET between donor and acceptor through acceptor saturation.[22] The modulation frequency is limited by the lifetimes of the states involved, making long-lived photoswitches[3,5] or chemically induced transitions[23] possible alternative schemes for slower signal recovery applications.

Circumventing the need for a dark state for modulation, all-optical methods of directly decreasing fluorescence intensity from the emissive level have recently been utilized for super-resolution imaging,[24–32] studying effects of fluorescence quenching on solvent-sensitive fluorophores,[33] and for detecting gain in the depletion laser from weakly emissive fluorophores.[34] Complementary to fluorescence modulation experiments,[20–22] secondary laser induced partial and repetitive optical depletion of the fluorescent state should also lead to strongly modulated fluorescence.[33] Thus, by implementing Stimulated Emission Depletion (STED) for fluorophore modulation, one should be able to repetitively suppress fluorescence at any desired modulation frequency. Herein, we demonstrate an all-optical approach to fluorescence image recovery by modulating the depletion laser intensity at any arbitrary frequency. By optically depleting the excited singlet population faster than the radiative rate, fluorescence is directly modulated, thereby enabling recovery of STED-modulated fluorescence. In this case, signal improvement relies on higher STED efficiency of the introduced fluorophore relative to background emitters.

II. Experimental

Alexa 594 hydrazine and crimson beads (Invitrogen) were used as received. Alexa 594 solutions were prepared by dissolution in deionized water (18 MΩ) followed by dilution to experimental concentrations. 200-nm and 20-nm crimson beads were each diluted 10-fold in an aqueous saturated poly(vinyl alcohol) (PVA) solution, followed by spin coating onto a coverslip at 1000 rpm. All dual laser experiments were performed on a microscope (Olympus IX71) using a 60x water immersion objective (Olympus 1.2 NA). All solution data was taken by focusing 25 microns into solution. Signal was collected in a confocal arrangement with a 50-μm multimode fiber serving as the pinhole and directing the emission to a photon-counting avalanche photodiode (APD, Perkin Elmer). Intensity trajectories were recorded using a National Instruments counting board controlled with Labview to time-stamp individual photon arrival times. All laser excitation was performed with ~6-ps pulses from a Ti:sapphire laser (745 nm, Coherent Mira 900) and a synchronously pumped optical

parametric oscillator (OPO, Coherent). The 1070-nm OPO output was doubled in BBO to provide the primary 535 nm excitation, while the Ti:sapphire output (at 745 nm) provided the depletion beam. The transverse mode was improved through coupling into a fiber or into a spatial filter prior to aligning into the microscope.

The two beams were overlapped spatially and temporally in the microscope after combining on a dichroic mirror. The depletion beam is delayed <100 ps after primary excitation. Continuous-wave primary (543 nm He-Ne) and modulated secondary (765 nm Ti:sapphire) laser excitation was also utilized to recover fluorescent images with STED modulation. Appropriate band pass filters were used to efficiently block both the primary excitation and the lower energy depletion laser, with an additional short-pass filter being used to fully block the higher power depletion beam. Mechanical choppers and an electro-optic modulator (Conoptics) were used to modulate the incident laser beams, with recorded time traces being oversampled (binned 10-fold faster than the modulation frequency) to show modulated fluorescence traces. Such square-wave modulation results in the fundamental and odd harmonics being observed in the frequency spectra. When CCD collection was used, frame rates were synchronized to the modulation frequency, but were also collected at 10 times higher frequency in an epifluorescence geometry with a larger (defocused) primary laser excitation area and a smaller, focused depletion laser spot. Images were processed by Fourier transformation of the time trace of individual pixel intensities to reveal the frequency components. The corresponding amplitude at the modulation frequency of each pixel was used to recover the demodulated image.[20–22]

NIH 3T3 cells were cultured in Dulbecco's Modified Eagle Medium (DMEM) supplemented with 10% fetal bovine serum (FBS). Cells were passaged and plated into 35mm glass-bottom dishes. Two days later, cells were fixed, permeabilized, and actin was labeled with AlexaFluor594-phalloidin (Invitrogen). Briefly, cells were rinsed with phosphate-buffered saline (PBS) and fixed with 3.7% formaldehyde for 10 minutes at room temperature. After washing 3 times with PBS, cells were permeabilized with 0.1% Triton X-100 for 5 minutes at room temperature. Cells were washed again 3 times with PBS. A dilution of 1:40 was made of the AlexaFluor594-phalloidin methanolic stock to PBS. Cells were stained with the diluted solution for 20 minutes at room temperature in the dark. Cells were washed 3 times with PBS to remove excess AlexaFluor594-phalloidin.

III. Results and Discussion

Adapting the STED concept, but with two well-overlapped, Gaussian-shaped beams, STED decreases fluorescence of the entire excited volume due to stimulated emission. As the secondary laser is of longer wavelength than is the collected fluorescence, the STED experiment becomes directly analogous to SAFIRe,[20–22] using the fluorescent level as the "dark" state analog of previous efforts (Figure 1). Essential for modulation, when the depletion laser is on, fluorescence is reliably suppressed, but the modulation depth tolerance enables working with lower intensities than necessary for super-resolution imaging.[30] Because the depletion laser decreases fluorescence, its modulation directly modulates the detected fluorescence, enabling facile demodulation-based image recovery in either confocal or wide-field imaging. As the timing requirements of STED are dictated by the fluorescence lifetime, this all-optical approach to SAFIRe further generalizes fluorescence image modulation, with potential utility in fast confocal sample scanning. Further, dye selection becomes more straightforward than for either SAFIRe[20–21] or Optical Lock-In Detection(OLID)[3] that require either long wavelength dark state transient absorbance or photoswitching donors in FRET pairs, respectively. For STED, photostability and high STED efficiency are the primary concerns.

Commonly used in STED imaging, both Alexa 594[29] and crimson fluorescent beads[29, 32] show excellent fluorescence suppression with low background to yield high-resolution images. The fluorescence of either fluorophore can be suppressed under both continuous wave (cw)[29] and pulsed excitation.[32] While the experimental setup using CW lasers is relatively simple and avoids two-photon excited background, average intensities of the depletion laser are lower using pulsed lasers to achieve the same modulation depth. Using Alexa 594, the incident intensity of the depletion laser was about 40% of that used with crimson beads to reach the same suppression of fluorescence signal. In accord with the ratio of fluorescence lifetime to interpulse period, ~80 MHz pulsed excitation requires ~3–4-fold lower intensities than with cw excitation.[32]

The 200-nm crimson beads spun cast in PVA were used to demonstrate the synchronous fluorescence image recovery using STED demodulation. The primary laser was a 543 nm He-Ne laser with 300 μW defocused to an area with diameter of ~8 μm, fwhm. The depletion (secondary) laser was a cw Ti:sapphire (Coherent Mira 900, 765nm, 30 mW). The secondary laser was chopped at 4Hz, enabling synchronous CCD detection at 40Hz frame rates. Figure 2A shows a raw epifluorescence image, in which the fluorescent beads were distributed throughout the excitation region. Each pixel intensity vs. time is Fourier transformed and the set of pixel amplitudes at 4Hz generate the demodulated image (Fig. 2B). Only the region illuminated by both lasers is recovered in Figure 2B, corresponding to the much smaller depletion laser-illuminated area (black circle in Fig. 2A). Comparing Figures 2A and 2B, the recovered image exhibited relatively weak raw fluorescence intensity. Nearby beads with two- to three-fold stronger intensity are not recovered in the demodulated image as they are not illuminated by the depletion laser. The time trace at the center of the recovered image is shown in Figure 2C, with a ~30% modulation depth.

PVA-immobilized crimson beads are useful in demonstrating the image recovery, but not necessarily relevant to most biological applications. Alexa594, however, is both an excellent STED fluorophore[29] and is commonly used in solution and for cellular labeling.[29] Allowing reduced average laser intensities, STED modulation of Alexa594 in aqueous solution was performed with spatially and temporally overlapped 80 MHz, ~6ps pulsed primary (700 W/cm^2) and depletion (200 kW/cm^2) lasers. For image modulation, the primary laser was defocused (2 μm fwhm). Since only the region in which the depletion laser is tightly focused yields depleted fluorescence, the out-of-focus fluorescence signals are also rejected, giving the ability to recover optical sections upon demodulation. The depletion laser was modulated at 6 Hz and the frame rate of the CCD camera was set to 60 Hz. A series of 3000 frames were recorded. Figure 3A shows one individual frame of the raw image, which shows the size of the defocused primary laser. After Fourier transformation of the time traces at each individual pixel and extracting the amplitude of the 6-Hz component, the demodulated image shows fluorescence only from the smaller, focused depletion laser-illuminated spot (Figure 3B).

As the timing requirements of STED are comparable to the fluorescence lifetime, the depletion laser can in principle be modulated at very high frequencies. To demonstrate this capability, the depletion laser was chopped at 20 Hz, 200 Hz and 2000 Hz. The fluorescence signal from Alexa 594 solution was collected with an APD and recorded in Labview. Binning at rates 10-fold higher than the modulation enables facile demodulation of Alexa emission (Fig. 4). At 20 Hz, the modulation of fluorescence intensity is clearly observed, varying between 220,000 to 340,000 counts/s for the depletion laser being on and off, respectively. Although the high modulation frequencies can be difficult to see in the raw intensity trajectories due to only moderate count rates, the modulation frequency components are readily revealed at all three modulation frequencies after Fourier transformation (Fig. 4D).

Often problematic for STED-based imaging, the high intensity depletion laser commonly generates undesired fluorescence via multiphoton excitation.[4] This two-photon excitation cannot be descriminated from the STED modulated signal. While the STED process suppresses the fluorescence, the two-photon excitation increases the total fluorescence intensity. Thus, in modulated STED, unwanted two-photon excitation of Alexa 594 similarly decreases the STED modulation depth, canceling out part of the fluorescence suppression by the depletion laser (Figure 5). The contribution of two-photon excitation does not change with the intensity of the primary laser. At lower primary excitation intensities, the desired depleted fluorescence just offsets and cancels out the out-of-phase two-photon excited fluorescence, causing an initial decrease in demodulated amplitude. Increasing the primary laser intensity increases the modulation amplitude without increasing background from the depletion laser alone, thereby enabling the STED component to dominate only at high primary laser intensities.

As the STED-offsetting two-photon-excited fluorescence cannot be spectrally discriminated from the depleted emission, this obscures both superresolution and signal recovery schemes. To minimize such signals in STED microscopy, one often must stretch the depletion laser pulse width to minimize undesirable two-photon excitation, complicating the experimental setup. Modulation, however, offers a more straightforward solution. Because the STED-modulated fluorescence intensity is linearly dependent on both the primary and the depletion laser intensities, only the STED-modulated fluorescence will be observed at the sum and difference frequencies. Using the sum or difference frequency components to construct the fluorescence image, the recovered image can be free from background induced by the primary or depletion lasers alone. Therefore, whether from background-generating fluorophores or from the STED dye of interest, two photon-excited fluorescence can be completely discriminated against through dual modulation.

In this manner, only those signals depending on both laser intensities are recovered, ensuring that no two-photon-induced fluorescence obscures the signals. Modulation of both primary (45 Hz, 40 W/cm^2) and depletion (~8 Hz, 550 kW/cm^2) lasers directly encodes both modulation frequencies on the collected Alexa 594 fluorescence (Fig. 6A, B). The frequency components at the sum and difference of the individual laser modulation frequencies contain only the fluorescence dependent on both beams exciting the sample. Such signal discrimination directly enables Alexa594 fluorescence recovery in solution (Fig. 7). After Fourier transform, the frequency components at the sum (Fig. 7B) and difference (not shown) frequencies reveal that only the focus of the depletion laser was imaged, demonstrating the capability of fluorescence recovery using dual modulation. Importantly, in contrast to the depletion-only modulation frequency (Fig. 5 & 6), the dual modulation frequency components at the sum and difference frequencies (Fig. 6) increase linearly with primary laser power, thereby discriminating against any depletion laser-induced two-photon signal or other signal-degrading background.

The intensity required for STED modulation/demodulation is relatively high, making confocal scanning a more suitable approach for cellular imaging. The capability of image recovery using modulated STED was demonstrated using Alexa594-labeled phalloidin within fixed NIH3T3 cells (Fig. 8). While the high primary laser intensity is favorable for reducing the impact of contrast-degrading two-photon-excitation, the possiblity of causing fast bleaching during the confocal scanning limits primary laser intensity. Both dual modulation (as demonstrated above) and appropriate combination of primary and depletion laser intensities can enhance modulation depth while minimizing both bleaching during scanning and contrast-degrading two-photon-excitation. The primary and secondary laser intensities of 40 W/cm^2 and 150 kW/cm^2, respectively, were used for the confocal scanning of the NIH3T3 cells. According to the results in Figure 5A, this combination provides

reasonable modulation depth and enables facile image recovery at the depletion laser modulation frequency when using the simpler depletion-only modulation, revealing positions of actin within the cells. Under these conditions, no significant bleaching was observed during the cell scanning. A sample scanning arrangement was used to maintain alignment and overlap of both laser spots during imaging. In each position, a series of modulated fluorescence signals were collected and demodulated via Fourier transform. Time-stamped photon arrival times are collected at each pixel, enabling both total counts and frequency components to be determined at every pixel in the image (Figure 8A). Comparison of the average and demodulated images shows that the background is reduced and the resolution in image 8B is also slightly improved, as would be expected from the linear intensity dependence of the demodulated STED fluorescence on both the primary and depletion lasers. This two-photon process has a slightly improved resolution over linear fluorescence microscopy. Although no effort was made to obtain sub-diffraction resolutions, one would expect the resolution to improve by ~1.4 due to sequential two-laser excitation. Line profiles (Figure 8C) further demonstrate this modest improvement, even with the large step size used (200 nm). The clear advantages of background removal and feature narrowing, however, result from dual laser illumination and image recovery.

Acknowledgments

The authors gratefully acknowledge support from NIH R01-GM068732.

Notes and references

1. Elgass K, Caesar K, Wanke D, Harter K, Meixner AJ, Schleifenbaum F. Anal Bioanal Chem. 2010; 398:1919–1925. [PubMed: 20811880]
2. Sun Y, Phipps J, Elson DS, Stoy H, Tinling S, Meier J, Poirier B, Chuang FS, Farwell DG, Marcu L. Optics Lett. 2009; 34:2081–2083.
3. Marriott G, Mao S, Sakata T, Ran J, Jackson D. Proc Natl Acad Sci USA. 2008; 105:17789–17794. [PubMed: 19004775]
4. Ramanujan VK, Zhang JH, Biener E, Herman B. Journal of Biomedical Optics. 2005; 10:0514071–0514011.
5. Hess ST, Gould TJ, Gudheti MV, Maas SA, Mills KD, Zimmerberg J. Proc Natl Acad Sci USA. 2007; 104:17370–17375. [PubMed: 17959773]
6. Elf J, Li GW, Xie XS. Science. 2007; 316:1191–1194. [PubMed: 17525339]
7. Kural C, Kim H, Syed S, Goshima G, Gelfand VI, Selvin PR. Science. 2005; 308:1469–1472. [PubMed: 15817813]
8. Sako Y, Minoghchi S, Yanagida T. Nature Cell Biology. 2000; 2:168–172.
9. Bates M, Huang B, Dempsey GT, Zhuang X. Science. 2007; 317:1749–1753. [PubMed: 17702910]
10. Betzig E, Patterson GH, Sougrat R, Lindwasser OW, Olenych S, Bonifacino JS, Davidson MW, Lippincott-Schwartz J, Hess HF. Science. 2006; 313:1642–1645. [PubMed: 16902090]
11. Cordonnier M, Uy D, Dickson RM, Kerr KE, Zhang Y, Oka T. J Chem Phys. 2000; 113:3181–3193.
12. Moerner WE, Kador L. Phys Rev Lett. 1989; 62:2535–2538. [PubMed: 10040013]
13. Bawendi MG, Rehfuss BD, Oka T. J Chem Phys. 1990; 93:6200–6209.
14. Weiss S. Science. 1999; 283:1676–1683. [PubMed: 10073925]
15. Orrit M, Bernard J. Phys Rev Lett. 1990; 65:2716–2719. [PubMed: 10042674]
16. Lin B, Urayama S, Saroufeem RMG, Matthews DL, Demos SG. Optics Express. 2010; 18:21074–21082. [PubMed: 20941003]
17. Chang WT, Yang YC, Lu HH, Li IL, Liau I. J Am Chem Soc. 2010; 132:1744–1745. [PubMed: 20102188]

18. Bierwagen J, Testa I, Folling J, Wenzel D, Jakobs S, Eggeling C, Hell SW. Nano Lett. 2010; 10:4249–4252. [PubMed: 20831171]
19. AUBIN JE. The Journal of Histochemistry and Cytochemistry. 1979; 27:36–43. [PubMed: 220325]
20. Richards CI, Hsiang JC, Senapati D, Patel S, Yu J, Vosch T, Dickson RM. J Am Chem Soc. 2009; 131:4619–4621. [PubMed: 19284790]
21. Richards CI, Hsiang JC, Dickson RM. J Phys Chem B. 2010; 114:660–665. [PubMed: 19902923]
22. Richards CI, Hsiang JC, Khalil AM, Hull NP, Dickson RM. J Am Chem Soc. 2010; 132:6318–6323. [PubMed: 20397664]
23. Szent-Gyorgyi C, Schmidt BF, Fitzpatrick JAJ, Bruchez MP. J Am Chem Soc. 2010; 132:11103–11109. [PubMed: 20698676]
24. Hell SW, Wichmann J. Optics Letters. 1994; 19:780–782. [PubMed: 19844443]
25. Fourkas JT. J Phys Chem Lett. 2010; 1:1221–1227.
26. Kuang C, Zhao W, Wang G. Rev Sci Instrum. 2010; 81:0537091–0537094.
27. Kasper R, Harke B, Forthmann C, Tinnefeld P, Hell SW, Sauer M. Small. 2010; 6:1379–1384. [PubMed: 20521266]
28. Moneron G, Hell SW. Optics Express. 2009; 17:14567–14573. [PubMed: 19687936]
29. Ding JB, Takasaki KT, Sabatini BL. Neuron. 2009; 63:429–437. [PubMed: 19709626]
30. Harke B, Keller J, Ullal CK, Westphal V, Schönle A, Hell SW. Optics Express. 2008; 16:4154–4162. [PubMed: 18542512]
31. Hell SW. Science. 2007; 316:1153–1158. [PubMed: 17525330]
32. Willig KI, Harke B, Medda R, Hell SW. Nature Methods. 2007; 4:915–918. [PubMed: 17952088]
33. Gryczynski I, Kusba J, Gryczynski Z, Malak H, Lakowicz JR. Journal of Physical Chemistry. 1996; 100:10135–10144.
34. Min W, Lu S, Chong S, Roy R, Holtom GR, Xie XS. Nature. 2009; 461:1105–1109. [PubMed: 19847261]

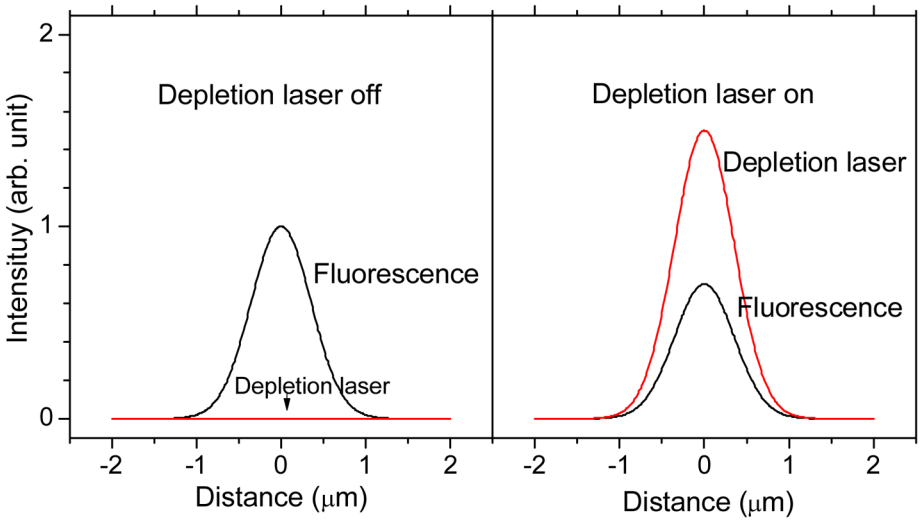

Figure 1.
Schematic of fluorescence modulation with the depletion laser. In the absence of signal-degrading, depletion laser-induced two-photon excited fluorescence, co-illumination with the depletion laser (right) suppresses fluorescence relative to no depletion laser co-illumination (left).

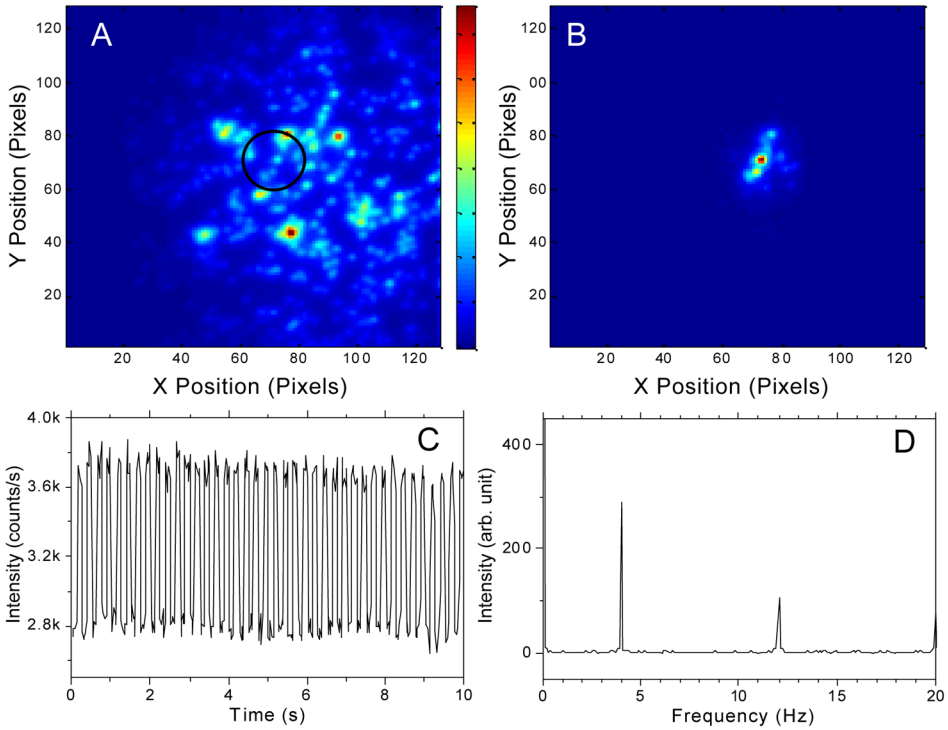

Figure 2.

The range of the image A and B: 16.7 μm × 16.7 μm. A. Raw image of an individual frame of 200-nm crimson beads immobilized in a PVA film imaged with Andor iXon CCD camera at 40 Hz. The primary laser is a defocused cw 543 nm He-Ne laser (5 kW/cm^2, ~8 μm fwhm). The black circle indicates depletion laser position (765 nm CW Ti-sapphire laser, 1.2 MW/cm^2, modulated at 4 Hz, ~1.6 μm fwhm). B. Demodulated image showing the extraction of the signal from the pixels that are simultaneously exposed to both lasers. C. Fluorescence trajectory from the central region exposed to both lasers. D. Fourier transform of the time trace in C. The modulation depth is ~30% as the constant offset on the CCD is ~1000 counts/pixel/frame.

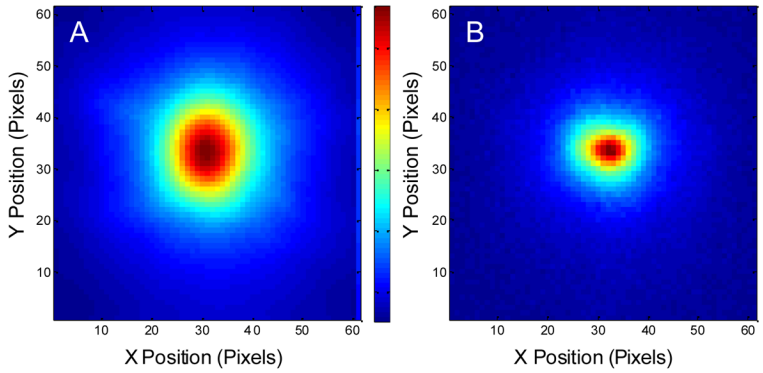

Figure 3.

Modulated Alexa 594 fluorescence in solution. The range of the images: 8 μm × 8 μm. A. Raw image of an individual frame of Alexa 594 solution fluorescence with defocused 535 nm pulsed excitation (~700 W/cm^2) and tightly focused 745 nm pulsed co-illuminating depletion laser (200 kW/cm^2) modulated at 6 Hz, coupled with synchronous CCD detection at 60 Hz. B. Demodulated image showing the extraction of the smaller region yielding signal from the pixels that are simultaneously exposed to both lasers.

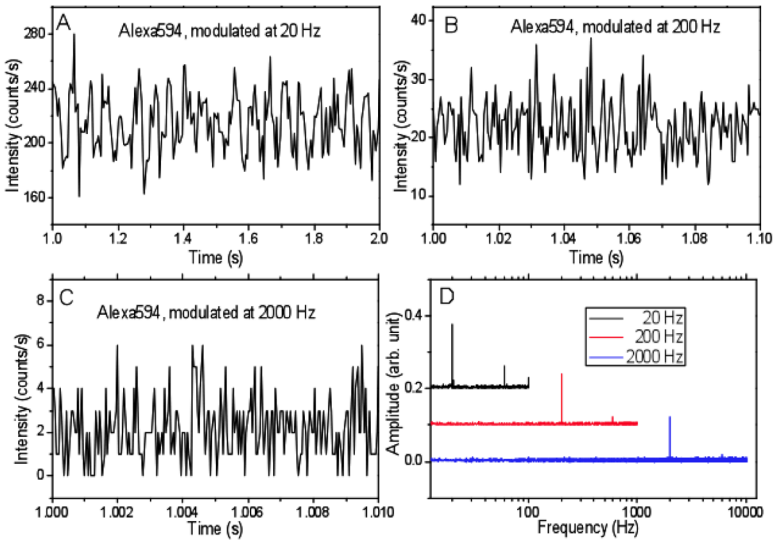

Figure 4.

Fluorescence of Alexa 594 solution collected with an APD in single-photon counting mode with constant 535 nm pulsed excitation and 745 nm pulsed depletion modulated at (A) 20, (B) 200 and (C) 2000 Hz. The intensities of the 535 nm and 745 nm pulsed lasers are 105 W/cm^2 and 150 kW/cm^2, respectively. (D) Fourier transform of the emission in (A–C), each binned an order of magnitude faster than the modulation.

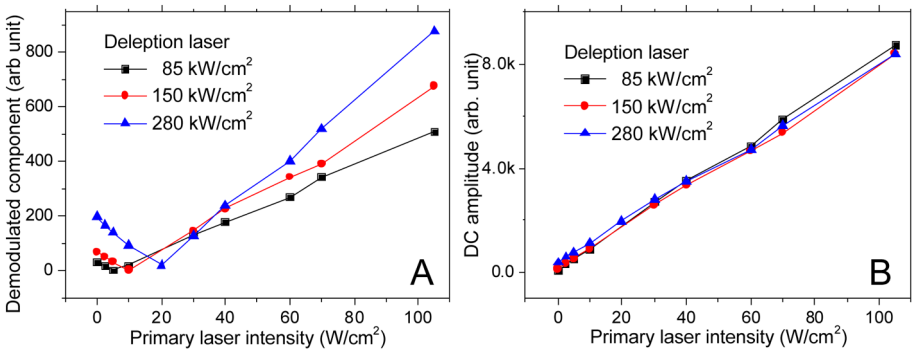

Figure 5.

Modulated Alexa 594 fluorescence in solution as a function of primary laser intensity. As the primary excitation increases, the STED fluorescence overcomes the constant depletion-laser-induced two photon excited fluorescence. A. Amplitude of the 10-Hz frequency component initially decreases, then increases as the signal-degrading two-photon excited fluorescence from the depletion laser is overcome by the STED signal. B. The DC (non-modulated) total fluorescence signal increases linearly with increasing primary laser intensity. Fluorescence from both primary and two-photon excited secondary laser excitation give rise to the signal in B. The STED component in A is seen to be out of phase, and offset by the degrading two-photon signal, when demodulated.

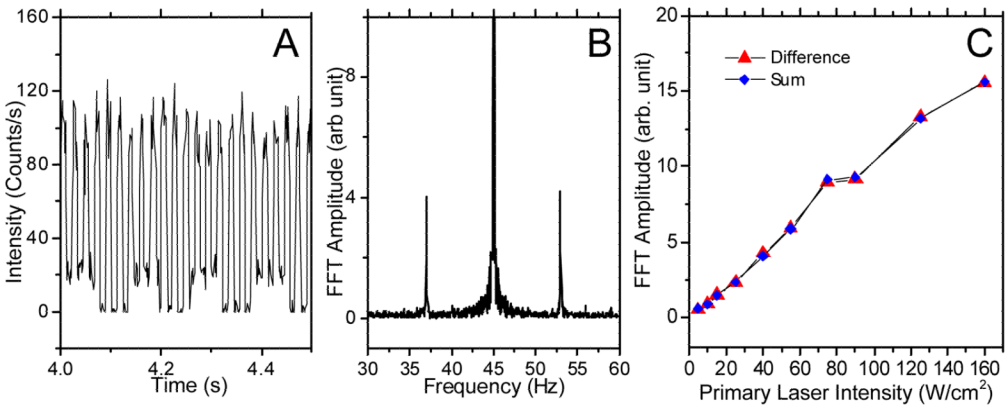

Figure 6.

Dual modulation STED. (A) The fluorescence emission of Alexa 594 solution with the depletion laser at 550 kW/cm^2 modulated at 8 Hz and with the primary laser at 40 W/cm^2 modulated at 45 Hz. (B) The sum and difference frequency side bands from dual modulation in the Fourier transform of the emission in (A). (C) The frequency components of Alexa 594 solution at the dual modulation difference (37 Hz, triangle) and sum (53Hz, diamond) frequencies as a function of primary laser power. The primary laser is at 535 nm modulated at 45 Hz and the depletion laser is at 745 nm modulated at 8 Hz.

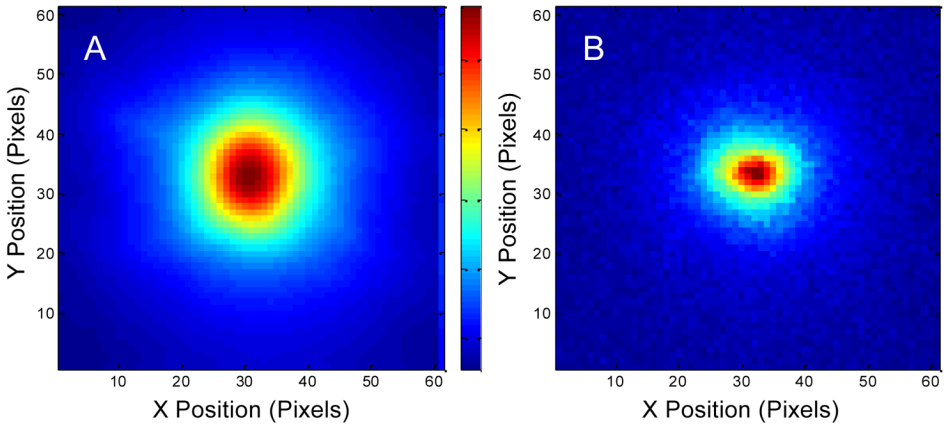

Figure 7.

Raw and demodulated images of Alexa 594 solution with modulation of both primary and secondary lasers. Primary laser is pulsed and defocused, with wavelength of 535 nm and power of ~700 W/cm^{2}μW, modulated at 5 Hz. The depletion laser is a tightly focused 745 nm laser with ~ 200 kW/cm^2 power, modulated at 6 Hz. The range of the images: 8 μm × 8 μm. A) One of the raw frames of Alexa 594 solution in dual modulation. B) Demodulated image at 11 Hz.

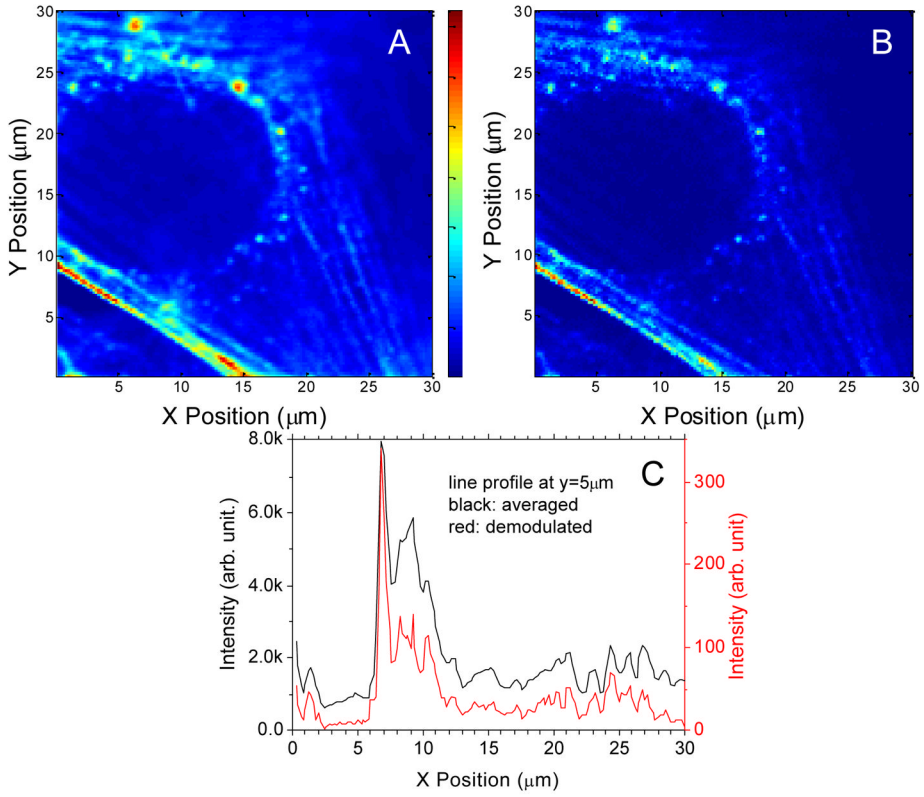

Figure 8.

Confocal scanning of NIH 3T3 cells using STED demodulation. A. The primary laser is 40 W/cm^2 at 535 nm. The depletion laser is 150 kW/cm^2 at 745 nm. Modulation frequency is 50 Hz. The range of the images: 30 μm × 30 μm. A. The averaged 3T3 image. B. The demodulated 3T3 image. C is the line profile of averaged and demodulated images at y = 5 μm.